Analysis of Lead Oxide (PbO) Layers for Direct Conversion X-Ray Detection

M. Simon, R. A. Ford, A. R. Franklin, S. P. Grabowski, B. Menser, G. Much, A. Nascetti, M. Overdick, M. J. Powell, and D. U. Wiechert

***Abstract*—Lead oxide (PbO) is a candidate direct conversion material for medical X-ray applications. We produced various samples and detectors with thick PbO layers. X-ray performance data such as dark current, charge generation yield and temporal behavior were evaluated on small samples. The influence of the metal contacts was studied in detail. We also covered large a-Si thin-film transistor (TFT)-plates with PbO. Imaging results from a large detector with an active area of 18 cm $\times$ 20 cm are presented. The detector has 960 $\times$ 1080 pixels with a pixel pitch of 184 μm. The modulation transfer function at the Nyquist frequency of 2.72 line-pairs/mm is 50%. Finally, a full size X-ray image is presented.**

***Index Terms*—Contacts, detective quantum efficiency, direct detection, lead oxide, PbO, X-ray detector.**

I. Introduction

SEVERAL years ago digital flat X-ray detectors based on amorphous silicon thin-film transistor (TFT)-plates were introduced in the market, e.g., to replace image intensifiers for dynamic X-ray imaging. Most of the existing products rely on *indirect* conversion where a scintillator (CsI) converts X-ray quanta into visible light, which is then detected by an array of photodiodes [1], [2]. An alternative detection scheme is a *direct* conversion [3] where X-rays absorbed in a semiconductor directly create electron hole pairs, which are subsequently separated by a bias field to generate a signal on the external electrodes. The benefits inherent of direct conversion are high spatial resolution and higher signal-to-noise ratio due to the higher charge generation yield of some materials. In addition, photodiodes production during plate fabrication is obviated. Drawbacks that have prohibited the success of direct conversion dynamic detectors so far include higher dark currents due to the high bias voltage needed, nonperfect temporal behavior, and the immaturity of the layer preparation procedure on an industrial scale.

Several materials are under investigation for direct conversion flat detectors. Best known is probably amorphous selenium, which has already gone into industrial production [4]. As X-ray detectors always need to cover a large area, *crystalline* semiconductors like cadmium zinc telluride (CZT) are still too expensive. Therefore, one has to concentrate on *polycrystalline* modifications of high-Z materials, the most promising candidates being HgI_2 [5], PbI_2 [6], poly-CZT [7] and PbO [8], [9].

First results on lead oxide from a small TFT-based detector were presented in 1998 [8]. More recently we carried out systematic material research on the one hand and on the other hand we developed an evaporation process, which has been scaled up for covering large-sized TFT-plates with thick PbO layers [9]. In this paper, we present new results on lead oxide with special focus on the influence of electrical contacts.

Manuscript received November 4, 2005; revised April 7, 2005.

M. Simon, S. P. Grabowski, B. Menser, G. Much, M. Overdick, and D. U. Wiechert are with the Philips Research Laboratories, 52066 Aachen, Germany (e-mail: matthias.simon@philips.com).

A. Nascetti was with Philips Research Laboratories, 52066 Aachen, Germany. He is now with the University of Rome "La Sapienza," Rome, Italy (e-mail: nascetti@mail.die.uniroma1.it).

R. A. Ford, A. R. Franklin, and M. J. Powell are with the Philips Research Laboratories, Surrey RH1 5HA, U.K.

Digital Object Identifier 10.1109/TNS.2005.856790

II. Experimental

A. Samples and Preparation of Layers

In our work we studied the basic physical properties of the material and established their relevance for X-ray conversion. We have produced detector demonstrators to evaluate the imaging performance of PbO-layers. We therefore used two different types of substrates during our investigations:

1) For the more material oriented research we designed special glass substrates of 2.5-in size and 1 mm thickness. 192 parallel strips of 0.2 mm $\times$ 38 mm area serve as bottom contacts. The strips were made of metal or indium-tin-oxide (ITO). These samples, referred to as "strip samples," were easy to fabricate and mount, and could thus be employed in large quantities. In addition they provide a one-dimensional spatial resolution and allow for a quick characterization of the material's X-ray performance.
2) Because the imaging performance of a PbO direct conversion detector cannot be evaluated on the one- dimensional strip samples, we evaporated PbO on a larger detector format. "Cardio"-sized plates, with an active area of 18 cm $\times$ 20 cm (960 $\times$ 1080 pixels, 184 μm size) were used to show the feasibility and imaging capability of PbO as a direct conversion material. The geometrical fill factor of the collecting electrodes is 80%. The scaling up of the evaporation process was a key point of our work. Our evaporation system can now be used for making a single large plate or four small strip samples simultaneously.

All PbO layers were prepared by direct evaporation process onto the substrate in a high vacuum chamber. PbO powder of 99.995% purity was heated in an especially designed evaporation cell. Crucible temperatures were in the range of 900–950 °C. We achieved growth rates of about 2 μm/min. Oxygen was supplied during the deposition in order to keep the growing layer stoichiometry. Water vapor was introduced in some cases. In general a substrate temperature of $T_{\mathrm{sub}} = 100^{\circ}\mathrm{C}$ was used. The equipment was capable of producing layers of

more than 300 μm "absorption thickness"[1] of 25 cm $\times$ 25 cm area. Metal top contacts were applied subsequently in a different vacuum chamber.

B. Basic X-Ray Properties—Definitions and Protocols

For X-ray measurements of the strip samples each strip was connected to a single channel of a low-noise charge-sensitive amplifier with a z-conducting contact mat. The top electrode, i.e., the homogeneous electrode opposite the strip (or pixel) side of the sample, was usually biased negatively with respect to the strips. All measurements were done with a standard medical tube (Philips SRM 0511) at 70 kVp and an internal filtration equivalent to 2.5 mm Al.

As several different measurement protocols and definitions are used in the field of detector physics, a short description of the three quantities follows, which we used for the initial characterization of our PbO layers.

1) Dark Current: For a given high voltage bias, a dark current flows through the detector. If the dark current is proportional to the bias voltage, the *dark resistivity* is well defined. However, several effects such as barriers at contacts may dominate the actual dark current of the layer-system rendering the voltage dependence non linear.

2) Charge Yield: From the signal during the X-ray pulse the dark current is subtracted, and the resulting value is divided by the absorption rate of X-ray energy. This quantity is called *charge yield* Y (unit: electrons/keV). The maximum possible charge yield is related to the energy W to create a single electron-hole-pair, which is also used in the literature: $W(\mathrm{eV}) = 1000/Y$.

3) Residual Signal: Several effects can lead to a retarded signal rise and a residual current after the end of the X-ray pulse [10], [11]. The residual signal current, or lag, is given as a percentage value of the current during the pulse. In this work we took the lag at 1 s after the end of a 5-s X-ray pulse as a measure for the temporal performance of the PbO layers. Other protocols were also implemented (e.g., using a single X-ray pulse of few milliseconds) leading to significantly smaller lag values than the ones presented here. However, we think that the first approach is more relevant for application purposes.

C. Imaging Performance of Detectors

Measurements of large area detectors took place in a specially designed test-setup, which allowed an easy and fast change of the panel under test. Detector characterization includes linearity measurement, detailed noise analysis, and noise power spectra (NPS). Two different approaches were used in order to determine the detector's spatial resolution, i.e., the modulation transfer function (MTF). First, using a thin slit (50 μm) in a tungsten piece [12], second, with a square wave object ("Huettner phantom") [13]. The detective quantum efficiency (DQE) was calculated according to [13]. The acquisition parameters for all measurements on large detector plates were: DN5 beam quality (70 kVp, 21 mm Al filter), 7 ms X-ray pulse duration, and a frame rate of 25 s^{-1}.

[1]"Absorption thickness" is the thickness of an equivalent layer of the full crystalline density and relevant for the X-ray absorption. The geometrical thickness depends on porosity and is around two times higher.

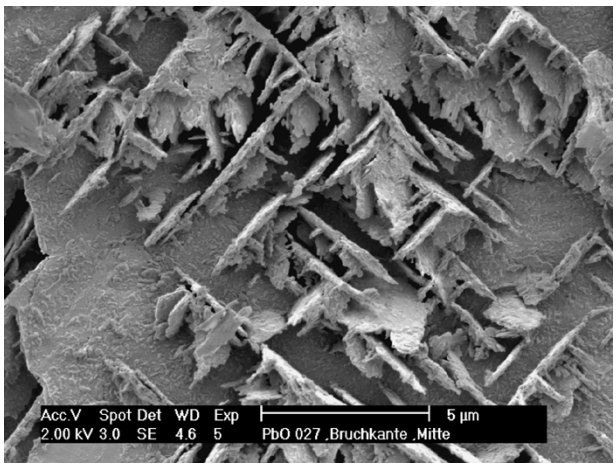

Fig. 1. Cross-section SEM-picture of a PbO-layer.

III. Physical Properties

We present first some basic physical properties of lead oxide. It exists in two polymorphic phases: a red tetragonal (α-PbO) and a yellow orthorhombic (β-PbO) phase. At room temperature the red phase is thermodynamically stable, yet the yellow phase also exists in a metastable state below the transition temperature of 490 °C. The two phases can be identified by X-ray diffraction or by Raman spectroscopy. Details of the Raman analysis of our layers can be found in a forthcoming publication [14].

Literature data as well as our own optical measurements reveal that PbO is a semiconductor with a bandgap of about 1.9 eV. Our layers are orange in color and consist of pure PbO but in both polymorphic phases. One has to distinguish between a thin seeding layer of less than 2 μm thickness and the bulk layer growth. Spatially resolved Raman spectroscopy of a cross section shows that the seeding layer is dominated by β-PbO, whereas the α-phase is the main constituent in the bulk.

The layers exhibit a very special microstructure, which is visible with a scanning electron microscope (SEM): the layers consist of very thin platelets of a few micrometer lateral dimensions and have a porosity of around 50% (Fig. 1). The full crystalline density would be 9.53 g/cm^3.

IV. X-Ray Properties

In this section we present the basic properties of PbO as X-ray conversion material, based on strip sample measurements.

A. Charge Yield

As one can see in Fig. 2 the charge yield increased with the bias voltage. This is the expected behavior, because the schubweg $s = \mu\tau E$ of the traveling charges increases with higher field. Saturation should be reached at high fields, which is not yet the case for the fields in Fig. 2. The theoretical electron–hole pair creation energy W in PbO can be calculated from Klein's rule [3] to be in the order of 6 eV. The theoretical limit for the charge yield Y is then 170 $\mathrm{e}^-/\mathrm{keV}$. A fit of the Hecht formula [15], although not fully applicable in the case of X-ray excitation, leads to effective $\mu\tau$-values of $4.4 \cdot 10^{-7}$ cm^2/V when irradiating the negatively biased electrode. Values of the same order of magnitude were found in a separate experiment

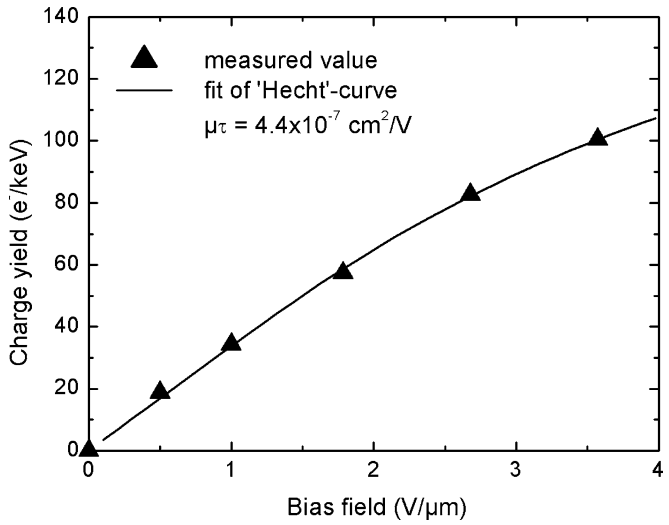

Fig. 2. Charge yield versus bias field with "Hecht"-fit curve.

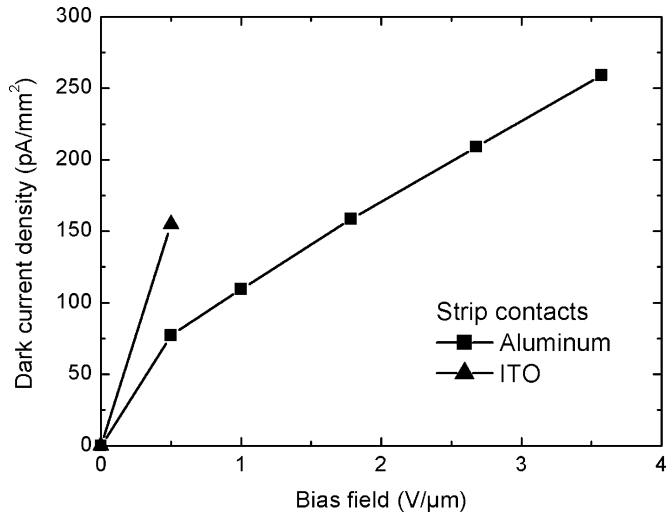

Fig. 3. Dark current density versus bias field for Al and ITO strip electrodes.

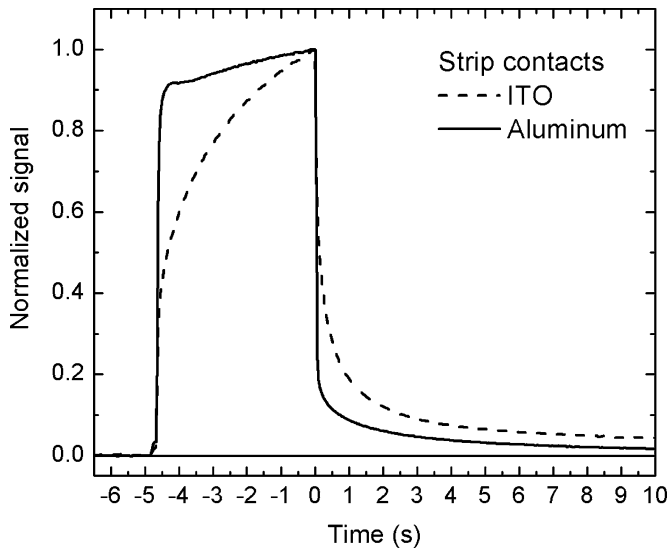

Fig. 4. Temporal behavior of signal current with Al and ITO strip electrodes.

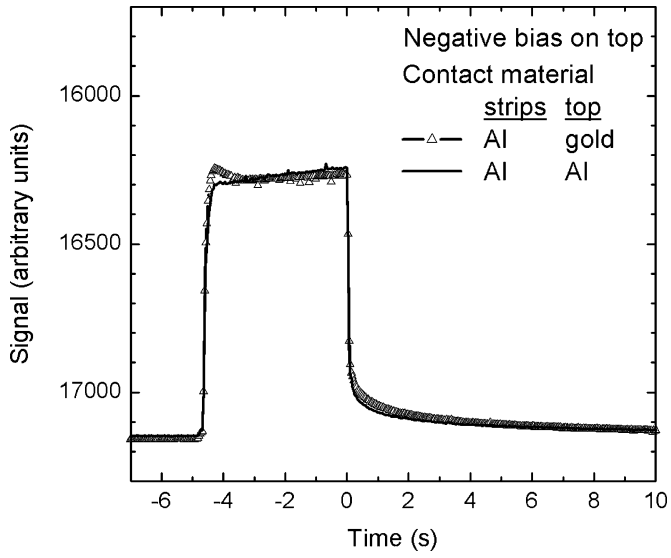

Fig. 5. Temporal behavior of signal current with **Al** strip contacts and **negative** bias of 2 V/μm at the top contact.

with blue light excitation for electrons and holes. The $\mu\tau$ values are not very high, but due to the very high resistivity of PbO, operating the device at elevated bias fields does not lead to unacceptably high dark currents.

B. Dark Current

In Fig. 3 the dark current density is plotted versus the bias field. For the aluminum strip contact, the dark current density is not strictly proportional to the bias field, the curve having some offset and a sublinear slope. The latter indicates the existence of blocking contacts in addition to a high bulk resistivity [16]. For the ITO strip contact, only one point has been measured, which exhibits twice the dark current at 0.5 V/μm bias field.

C. Temporal Behavior

Again comparing samples with aluminum and ITO strip electrodes, a strong influence of the contact material on the temporal behavior is observed. In Fig. 4 the response to an X-ray illumination of 5 s duration is shown. The sample with ITO strip electrode has a very slow signal rise and a high residual signal. To analyze this effect further, all combinations of gold and aluminum as strip or top electrode and under both bias polarities were measured (Figs. 5–8). Figs. 5 and 6 show the response curves for the negatively biased top electrode. The response during the X-ray pulse and the residual signal are better for the aluminum strip electrode than for the gold electrode. The material of the top electrode appears to have only little influence. This is different under a positive top electrode bias (Figs. 6 and 7), where the role of the top electrode material becomes dominant, again with the aluminum clearly giving the better temporal response. The difference between aluminum and gold in this case is even larger than for the positively biased strip electrodes.

Summarizing these and other experiments with different electrode materials, the temporal behavior of the PbO detector is strongly influenced by the electrode material on the positively biased side of the PbO. For positive electrodes made from less noble metals a better temporal response was consistently observed, while the material on the negative contact side had no

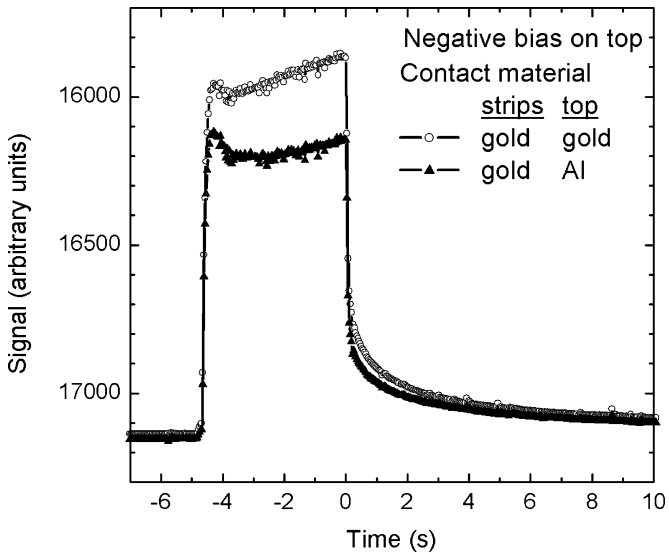

Fig. 6. Temporal behavior of signal current with **gold** strip contacts and **negative** bias of 2 V/μm at the top contact.

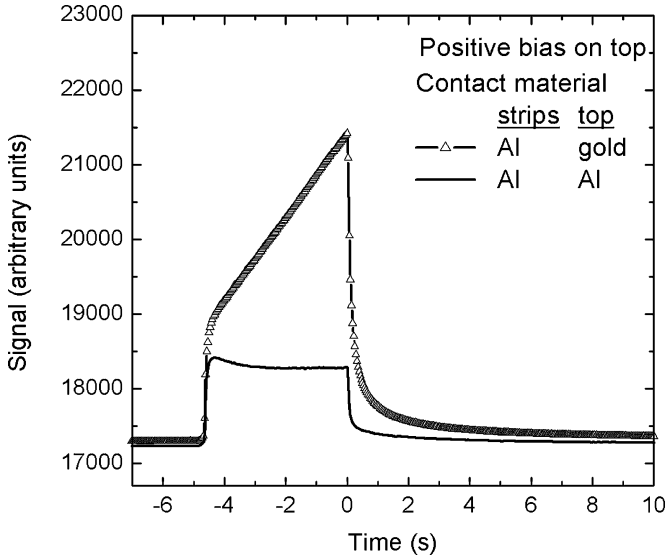

Fig. 7. Temporal behavior of signal current with **Al** strip contacts and **positive** bias of 2 V/μm at the top contact.

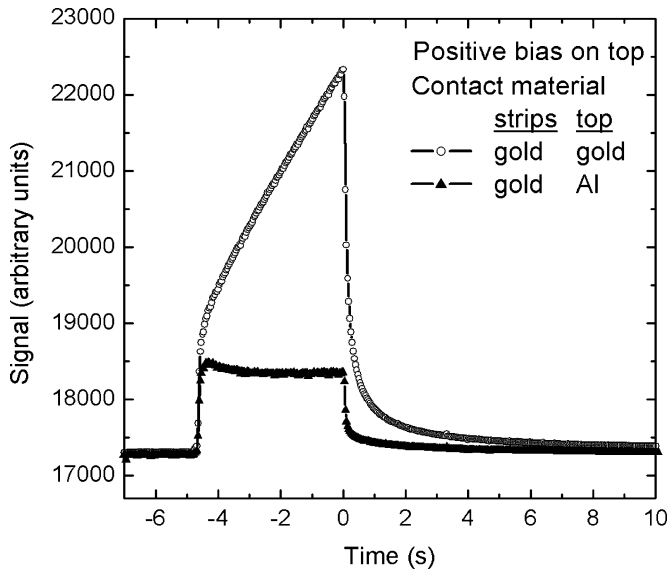

Fig. 8. Temporal behavior of signal current with **gold** strip contacts and **positive** bias of 2 V/μm at the top contact.

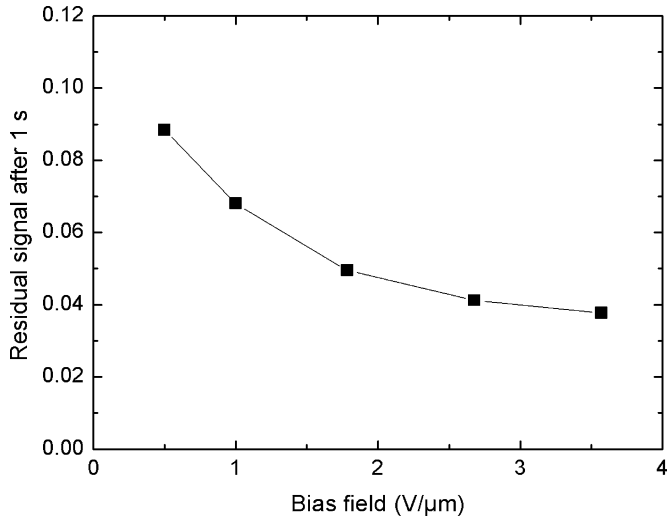

Fig. 9. Residual signal versus bias field for aluminum strip contacts.

significant influence. A possible explanation is the generation of electron accumulation layers induced in the PbO near a noble positive electrode by the X-ray signal, that leads to hole injection from this electrode. After the X-ray pulse ends, this charge injection continues until the charge accumulation layer eventually dissolves.

It should be noted, that the strip samples are not symmetric with respect to the electrodes. On one hand the microscopic interface between metal and PbO is different because the PbO growth takes place on the strips' smooth metal surface whereas the top metal contact is evaporated on the rather rough PbO surface. On the other hand the geometry of the electrodes differ a lot. The top electrode is not structured whereas the strips are separated by 10–20-μm-wide gaps. For these reasons the local electric field and electronic trap levels are supposed to be different for the strip and top contacts leading to a nonsymmetrical behavior.

The residual signal after the X-ray pulse also depends on the applied bias field. As shown in Fig. 9 for aluminum strips, the residual signals decrease from 9% at 0.5 V/μm to about 4% at 3.5 V/μm. The measurement conditions were a 5-s X-ray illumination at a dose rate of 680 μGy/s. For lower dose rates, higher residual signal values were found [9].

V. Large Plates: Imaging Performance

In the following an analysis of the imaging performance of one of the large TFT-plates covered with PbO is presented. The absorption thickness (i.e., the thickness if the PbO was not porous) of this layer was 160 μm, the geometrical thickness was 340 μm. More details of this analysis can be found in an earlier publication [9].

Linearity of detector response for X-ray dose values from 180 nGy up to 4.2 μGy/frame was verified for different bias values. Noise analysis of dark frames performed at 1 V/μm lead to noise values as low as 1800 electrons/pixel. Due to the high

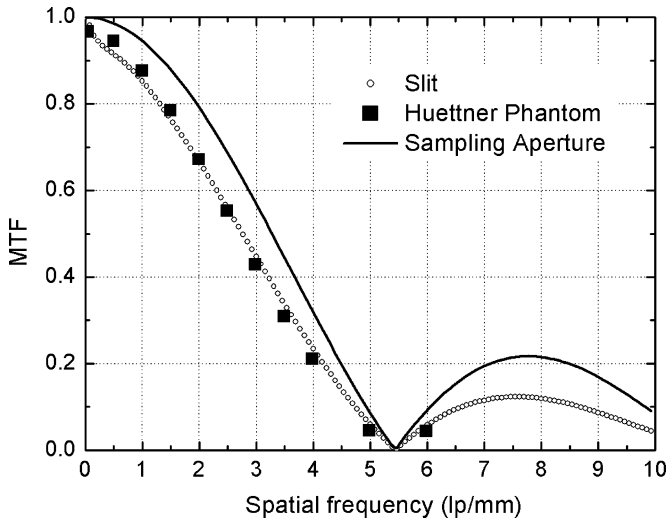

Fig. 10. Modulation transfer function (MTF) measured with two methods. The spatial frequency is given in linepairs (lp) per mm.

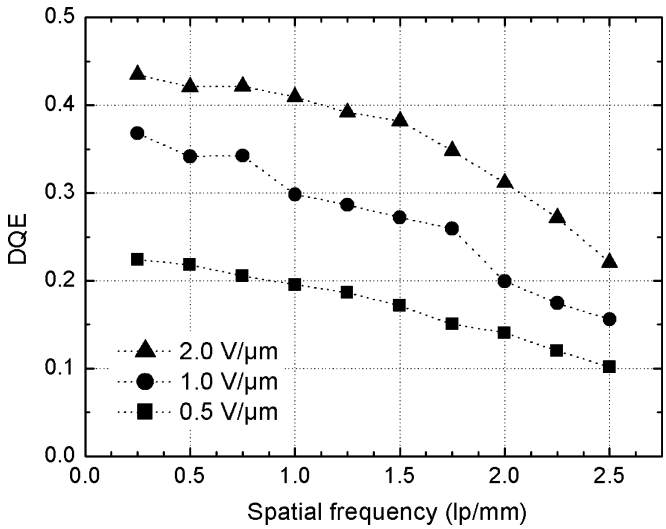

Fig. 11. DQE for different bias fields.

resistivity of PbO, the dark current shot noise contributes only 300 electrons/pixel to the pixel noise. All noise power spectra were corrected for lag effects [17].

Results of both methods used for the MTF-measurement are shown in Fig. 10 together with the sinc-function corresponding to the pixel pitch. A good agreement between the results of the two methods is achieved. The fact that the measured detector MTF is close to the theoretical sinc-function, even beyond the sampling frequency at 5.4 lp/mm, indicates a very high spatial resolution, i.e., the MTF of the PbO conversion layer itself is close to unity. This makes PbO a very attractive material for smaller pixel sizes, where the indirect conversion approach is limited due to light spread in the scintillator layer. It can also be observed that the position of the zero of the measured MTF coincides with the inverse of the pixel pitch, indicating an effective fill-factor of 1.

Finally, we calculated the DQE of the detector. The results are shown in Fig. 11 where DQE values for different bias fields are plotted. The DQE(0) expected from the thickness of the PbO layer (160 μm) is 0.65: the discrepancy of the measured DQE at low spatial frequency to the theoretical value could be related to NPS deterioration due to depth-dependent charge collection [18]. The DQE improvement with the increasing bias field can then be ascribed to the increase of the schubweg, which leads to a reduced depth dependency of the signal.

A full resolution image (960 $\times$ 960 pixels) showing a 'Huettner' phantom and a human hand phantom is reported in Fig. 12. The image is an average over 10 offset, gain and defect corrected frames acquired at 25 Hz frame rate with an X-ray dose of about 4 $\mu\mathrm{Gy/frame}$. High contrast objects as well as fine bone structures can be clearly distinguished.

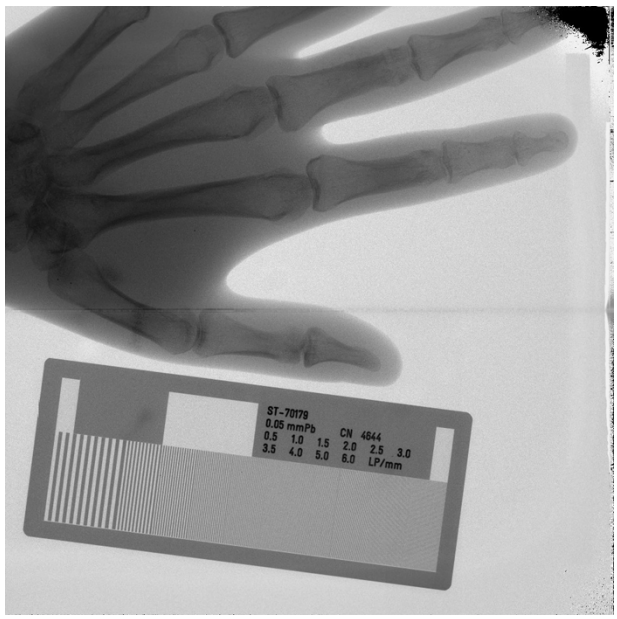

Fig. 12. X-ray image from a large detector.

VI. Conclusion

PbO is a promising candidate as direct X-ray converter for static as well as for dynamic applications. Strip samples were used to evaluate basic properties such as dark current, charge yield and temporal behavior. PbO exhibited a low dark current density even at high bias fields. The measured charge yield was sufficient for low dose imaging but still lower than the theoretical value of about 170 e^- keV. We found that the temporal behavior of the PbO detector depends strongly on the contact material, especially at the positive electrode. This topic needs to be studied further also to decrease the amount of residual signals.

The imaging performance of PbO-based X-ray detectors was analyzed using large area 18 cm $\times$ 20 cm TFT arrays. MTF measurements reveal that the PbO detector exhibits an effective fill-factor close to unity. Furthermore, the same measurements demonstrate the very high spatial resolution that can be achieved with PbO, making it very attractive for high-resolution detectors. The lower than expected DQE is attributed to incomplete charge collection at the bias fields used in the experiments.

REFERENCES

[1] F. Busse, W. Rütten, B. Sandkamp, P. L. Alving, R. J. M. Bastiaens, and T. Ducorant, "Design and performance of a high-quality cardiac flat detector," in *Proc. SPIE*, vol. 4682, 2002, pp. 819–827.

[2] P. R. Granfors, D. Albaglib, J. E. Tkaczykb, R. Aufrichtig, H. Netela, G. Brunsta, J. Boudrya, and D. Luoa, "Performance of a flat panel cardiac detector," in *Proc. SPIE*, vol. 4320, 2001, pp. 77–86.

[3] S. O. Kasap and J. A. Rowlands, "Direct-conversion flat-panel X-ray image sensors for digital radiography," *Proc. IEEE*, vol. 90, no. 4, pp. 591–604, 2002.

[4] D. C. Hunt, O. Tousignant, and J. A. Rowlands, "Evaluation of the imaging properties of an amorphous selenium-based flat panel detector for digital fluoroscopy," *Med. Phys.*, vol. 31, no. 5, pp. 1166–1175, 2004.

[5] G. Zentai, L. Partain, R. Pavlyuchkova, C. Proano, B. N. Breen, A. Taieb, O. Dagan, M. Schieber, H. Gilboa, and J. Thomas, "Mercuric iodide medical imagers for low exposure radiography and fluoroscopy," in *Proc. SPIE*, vol. 5368, 2004, pp. 200–210.

[6] G. Zentai, L. Partain, R. Pavlyuchkova, C. Proano, G. Virshup, P. Bennet, K. Shah, Y. Dmitriev, and J. Thomas, "Improved properties of PbI_2 X-ray imagers with tighter process control and using positive bias voltage," in *Proc. SPIE*, vol. 5368, 2004, pp. 668–676.

[7] S. Tokuka, H. Kishihara, S. Adachi, and T. Sato, "Improvement of the temporal response and output uniformity of polycrystalline CdZnTe films for high sensitivity X-ray imaging," in *Proc. SPIE*, vol. 5030, 2003, pp. 91–100.

[8] A. Brauers, N. Conrads, G. Frings, U. Schiebel, M. J. Powell, and C. Glasse, "X-ray sensing properties of a lead oxide photoconductor combined with an amorphous silicon TFT array," *Proc. Mat. Res. Soc.* , vol. 507, pp. 321–326, 1998.

[9] M. Simon, R. A. Ford, A. R. Franklin, S. P. Grabowski, B. Menser, G. Much, A. Nascetti, M. Overdick, M. J. Powell, and D. U. Wiechert, "PbO as direct conversion X-ray detector material," in *Proc. SPIE*, vol. 5368, 2004, pp. 188–199.

[10] W. Zhao, G. DeCrescenzo, and J. A. Rowlands, "Investigation of lag and ghosting in amorphous selenium flat-panel X-ray detectors," in *Proc. SPIE*, vol. 4682, 2002, pp. 9–20.

[11] M. Overdick, T. Solf, and H.-A. Wischmann, "Temporal artefacts in flat dynamic X-ray detectors," in *Proc. SPIE*, vol. 4320, 2001, pp. 47–58.

[12] H. Fujita, D. Y. Tsai, T. Itoh, K. Soi, J. Morishita, K. Ueda, and A. Ohtsuka, "A simple method for determining the modulation transfer function in digital radiography," *IEEE Trans. Med. Imag.*, vol. 11, no. 1, pp. 34–39, Jan. 1992.

[13] K. Stierstorfer and M. Spahn, "Self normalizing method to measure the detective quantum efficiency of a wide range of X-ray detectors," *Med. Phys.*, vol. 26, no. 7, pp. 1312–1319, 1999.

[14] D. U. Wiechert, S. P. Grabowski, and M. Simon, "Raman spectroscopy of PbO layers," *Thin Solid Films*, vol. 484, pp. 73–82, 2005.

[15] K. Hecht, "Zum Mechanismus des lichtelektrischen Primärstromes in isolierenden Kristallen," *Zeitschrift für Physik*, vol. 77, pp. 235–245, 1932.

[16] R. H. Bube, *Photoelectric Properties of Semiconductors*. Cambridge, U.K.: Cambridge University Press, 1992.

[17] F. Busse, W. Rütten, H.-A. Wischmann, B. Geiger, M. Spahn, R. J. M. Bastiaens, and T. Ducourant, "Methodology to measure fundamental performance parameters of X-ray detectors," in *Proc. SPIE*, vol. 4320, 2001, pp. 287–298.

[18] J. G. Mainprize, D. C. Hunt, and M. J. Yaffe, "Direct conversion detectors: the effect of incomplete charge collection on detective quantum efficiency," *Med. Phys.*, vol. 29, no. 6, pp. 976–990, 2002.